

# Forming Limit Investigation of AA6061 Friction Stir Welded Blank in a Single Point Incremental Forming Process: RSM Approach

Iman Alinaghian<sup>1</sup> · Hossein Ranjbar<sup>2</sup> · Mohammad Ali Beheshtizad<sup>3</sup>

Received: 25 March 2016 / Accepted: 8 March 2017 / Published online: 4 April 2017  
© The Indian Institute of Metals - IIM 2017

**Abstract** In the present work, an experimental study was made to identify formability characteristics of aluminum 6061 friction stir welded blank in an incremental forming process. Forming limit diagram, bowl height, minimum thickness and thickness distribution were studied to find formability of tailored welded blank. Firstly, series of experiments were carried out to find which joining direction caused higher formability and desired forming limit curve. For this purpose, joints with three different directions (i.e. rolling direction, transverse direction and diagonal direction) were prepared and formability i.e. formed bowl height until failure along with forming limit curves were compared. After finding the best joining direction, effect of welding process parameters i.e. rotational speed, plunge depth and travel speed on formability of welded blanks were analyzed by using response surface methodology (RSM). The results were discussed according to microstructure and fractography analysis obtained by scanning electron microscopy. After finding the effects, welded blanks with optimal parameter combination were fabricated and effect of incremental forming parameters i.e. spindle speed, feeding rate and axial step on thickness distribution were analyzed. Here, RSM was also used to find parametric and optimum setting of parameters. From

the results, it was obtained that joints with diagonal direction caused higher value of bowl height. Also, tool rotary speed of 1600 RPM, travel speed of 40 mm/min and plunge depth of 0.15 mm caused higher value of bowl height implying high formability. Furthermore, it was found that selection of 0 RPM spindle speed, 600 mm/min feeding rate and axial depth of 0.6 mm resulted in higher thickness distribution.

**Keywords** Tailored welded blanks · Friction stir welding · Formability · Single point incremental forming

## 1 Introduction

Welded blanks are used most commonly in automotive and marine industries because they significantly reduce the weight of structure and causes the vehicle to be fuel-efficient. Firstly, steels were used as tailor welded blanks and its application was extended as an effective way to reduce weights. However, for further reduction of structure weight, many manufacturers replaced aluminum alloys instead of steel to satisfy the fuel-efficiency and cost of the products. The application and development of tailor welded blanks (TWBs) of aluminum alloys is an applicable way of the vehicle weight reduction process [1–3].

Welding aluminum alloys by fusion welding process results in reduction of formability due to defects and a heterogeneous microstructure caused by melting of parent material and producing brittle intermetallic structures [4]. Hence, due to enhancement of the formability of TWBs similar to base metal, friction stir welding (FSW) is a favorable joining process for the production of tailor welded blanks, because it can make defect-free welds with a

✉ Mohammad Ali Beheshtizad  
mohammadali.beheshtizad@outlook.com

<sup>1</sup> Faculty of Mechanical Engineering, University of Kashan, Kashan, Iran

<sup>2</sup> Department of Mechatronics Engineering, Science and Research Branch, Islamic Azad University, Tehran, Iran

<sup>3</sup> Department of Computer Engineering, Shahrood Branch, Islamic Azad University, Shahrood, Iran

homogeneous microstructure in most metallic materials [5–9].

In recent past, the formability of aluminum based TWBs produced by friction stir welding process was attended by various researchers. In this matter, Sato et al. [10] analyzed formability of AA5052 welded blanks regarding variation of grain size. They used one directional tensile test and developed forming limit diagram for welded specimens and compared with that of base material. Results showed that fracture limit strain of plane strain deformation increased with increasing microstructure size in the stir zone. Hirata et al. [11] analyzed effects of microstructure of FSP region on formability of AA5083 blanks through both hydraulic bulging test and uniaxial tension test. They showed that joints with coarser grain distribution in the nugget had higher formability. Also, the results obtained by uniaxial tension test were completely in line with those derived through bulging test. Kim et al. [12] analyzed effects of joining material directions on the formability of friction stir welded AA6111 joints. They analyzed the results through uniaxial tension test, limit dome height test with hemispherical punch and Marcianiak cupping test. Results indicated that joints with arrangements in line with rolling directions had the highest formability. The obtained results were completely similar to all aforementioned formability tests. Ramalu et al. [13] analyzed effects of diameter of tool shoulder and plunging depth on formability of AA6061 joints through determination of forming limit diagram (FLD), thickness distribution and work hardening coefficient by means of uniaxial tension test. Their research findings indicated that the FLD of AA6061 joints was higher than that of base metal. Furthermore, they found that increase in tool shoulder diameter and plunge depth increased the formability and moved up the FLD diagram. Ahmadnia et al. [14] applied longitudinal ultrasonic vibration to FSW tool and analyzed the effect of vibratory tool on formability of AA6061 TWB by means of Erichsen cupping test. The results indicated that applying vibration with high power caused material softening and removed dislocations thus improving the formability.

The welded blanks due to existing irregularity of mechanical properties (due to presence of weld line and anisotropy) and heat affected zone has lower strength with respect to base metal. Therefore, for improving formability of TWBs, imposition of a localized forming process that forms the blank incrementally, is necessary, specifically in regions such as heat affected zone and weld nugget. Therefore, single point incremental forming is a suitable process for improving formability of TWBs. Silva et al. [15] performed a feasibility study to use single point incremental forming (SPIF) for forming pyramidal shapes from TWBs and showed that the combination of SPIF with tailored welded blanks produced by FSW seemed

promising in the manufacture of complex sheet metal parts with high depths. However, having a detailed knowledge about formability of TWBs by SPIF and effect of welding and forming process on forming behavior appropriately have not been reported so far.

In the present study an attempt is made to use SPIF for analyzing formability of welded blanks, those produced by friction stir welding process. Firstly, a series of experiments have been carried out to find effect of joining material direction on formability (i.e. height of formed bowl). After finding the best joining direction, a study has been performed based on RSM to find effect of welding parameters such as tool rotary speed, travel speed and plunge depth on forming height. After finding optimum welding parameter, welded blanks with optimum parameters have been fabricated and then RSM has also been used to find and analyze the effect of incremental forming process factors i.e. spindle speed, feeding rate and axial step on thickness distribution.

## 2 Experimental

### 2.1 Materials and Equipment

To fabricate 2 mm thick TWB with dimension of 250 mm × 250 mm, rolled plates of aluminum 6061 were cut into the required sizes by means of a hacksaw cutter. The chemical compositions and mechanical properties of base metal are presented in Tables 1 and 2, respectively. During FSW process, the plates were secured to by means of a clamping device. According to the literatures [7] and researches done in the laboratory, a tool with square pin profile, made of AISI H13 steel were used to fabricate the joints. This tool pin profile was selected due to its better stirring action and better material flow that enhanced the material flow and improved the weld strength. The four edge shapes of the tool pin caused better shearing of

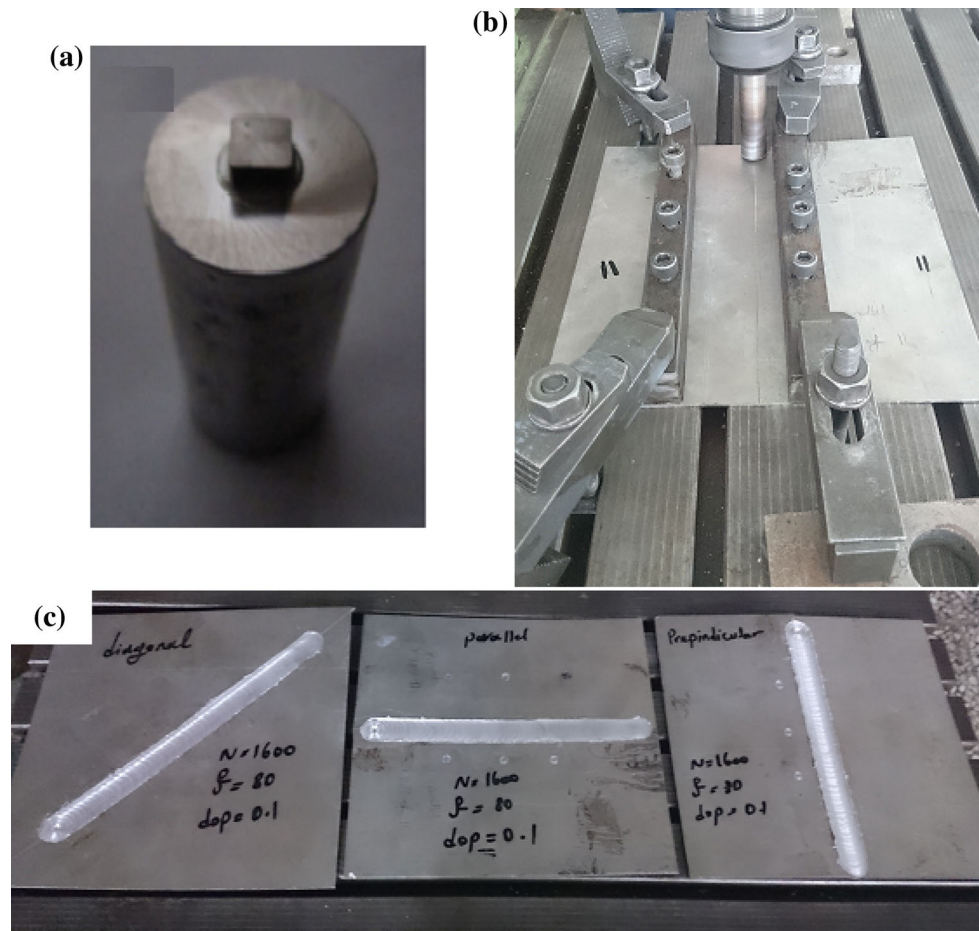
**Table 1** Chemical compositions of AA6061-T6

Components	Mg	Si	Fe	Cu	Cr	Mn	Zn	Ti	Al
Percents (%)	0.9	0.62	0.33	0.28	0.17	0.06	0.02	0.02	Bal

**Table 2** Mechanical properties of AA6061-T6

Description	Values
Yield strength (MPa)	302
Ultimate tensile strength (MPa)	334
Elongation (%)	18
Hardness (VHN)	125

**Fig. 1** FSW tool with square pin profile, experimental setup including sheets and clamp along with fabricated joints



material during its rotation and improved stirring action [16]. Although the square pin profile resulted in high tool wear, but due to its effect on joint strength, the square tool was used. The FSW setup including the clamping system and the fabricated tool was mounted on 4301 TABRIZ milling machine with maximum spindle speed of 5000 RPM and power of 15 hp. Figure 1 demonstrates FSW setup attachments along with fabricated joints.

After fabrication of welded blanks, in order to study their formability, incremental forming process was utilized to form them to bowl shape parts. A 5 axis CNC machine with SIEMENS controller was used here to form bowl products from welded blanks. An incremental forming tool with hemispherical tip and 10 mm radii was utilized to form the bowls.

The height of the bowl, until occurrence of failure like tear, was considered as a main criterion for formability. This value (i.e. forming height) could be recorded by controller of CNC machine exhibiting the value on its monitor. Figure 2 depicts incremental forming apparatus and formed parts.

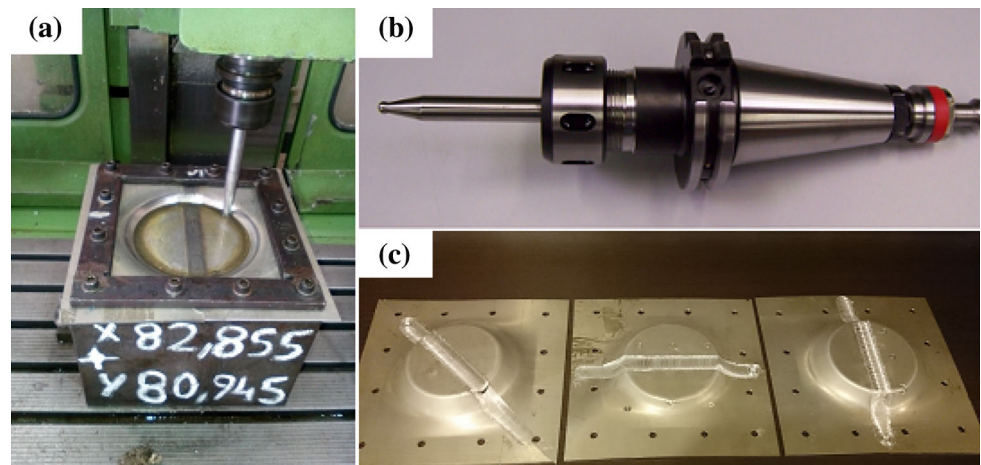
Also, the thickness distribution of the formed parts was measured by means of the digital micrometer. The formed

part was wirecut cross sectionally and the thickness distribution was measured. A 3D component KISTLER dynamometer model 9250B was utilized to monitor the forces acting during incremental forming process. A digital thermometer was also used to monitor and record the temperature history during FSW process.

Tensile tests on specimen from the weld region was carried out according to ASTM-E08 at a nominal cross-head speed of 1 mm/min and at room temperature to obtain strain hardening exponent. Temperature and the strain hardening coefficient ( $n$ ) values were evaluated as per the standard procedure after testing the samples till failure. The load-stroke behavior obtained during testing was converted into engineering stress–strain and true stress–strain behavior. The strain hardening exponent ( $n$ ) value was calculated from the slope of the natural logarithm plot of true stress and true strain ( $\ln \sigma$ – $\ln \epsilon$ ) in which the  $\sigma$ – $\epsilon$  values in the plastic deformation region were considered. The same procedure was repeated for all the combinations of joint direction and FSW parameter.

In order to examine the fractographic characteristics of the specimens, they were sectioned to the required sizes from the joints comprising nugget zone and then

**Fig. 2** Incremental forming setup including die and tool along with formed bowls



polished by using various grades of emery papers and finally by  $\text{Al}_2\text{O}_3$  suspension. Afterward, the polished samples were etched using a 4 ml  $\text{HNO}_3$ , 3 ml HD, 2.5 ml HCl and 200 ml  $\text{H}_2\text{O}$  to show the microstructure. Microstructural analysis was carried out using a light optical microscope, Mitutoyo with  $400\times$  resolution. Further, the fracture locations of the formed bowls were examined by Scanning Electron Microscope (TESCAN SEM). The fracture zone of the formed samples in  $10\text{ mm} \times 10\text{ mm}$  size parts were cut from the failure specimen and SEM images were taken from the removed portions.

## 2.2 Procedure and Method

In the present study, firstly a series of FSW experiment was performed to fabricate TWBs with high strength. By conducting these preliminary experiments, it was found that the joint which was fabricated by parameter setting of 1200 RPM tool rotary speed, 60 mm/min travel speed and 0.1 mm plunge depth had ultimate tensile strength of 220 MPa that was close to 70% of base metal. In order to find the appropriate welding parameter for evaluation of the effect of joint direction, a set of FSW experiments was carried out by varying tool rotation (800, 1200 and 1400 RPM), travel speed (20, 40 and 60 mm/min) and plunge depth (0.1, 0.15 and 0.2 mm). Figure 3 illustrates effect of FSW predominant factors on joint strength. It was found from Fig. 3a that increase in tool rotary speed from 800 to 1200 RPM, resulted in sufficient heat input, thus leading to enhanced material flow and stirring action and improved joint strength. On the other hand, when the tool rotation went beyond a critical value and reached 1400 RPM, due to high heat input the heat affected zone is excessively softened and lowers the joint strength. Also, it is seen from Fig. 3b that increase in travel speed resulted in increase in weld strength. For aluminum alloys, low travel speed

enhanced concentration of heat in FSP region and made the material soft. Hence, by increase in travel speed, cooling rate enhanced thus preventing softening of heat affected zone and enhanced the joint strength. Furthermore, it is clear from Fig. 3c that increase in plunge depth from 0.1 to 0.15 mm resulted in an increase in weld strength; while by further increase in plunge depth, the tensile strength decreased. By increase in plunge depth, due to induction of higher axial force, the weld line was pressed by plunging action and widened in cross section. These resulted in enhancement of joint strength during welding. However, plunge depth beyond a critical value, creates excessive material softening. This resulted in thinning of FSP region thus leading to a reduction in joint strength. Therefore, all the TWBs for first stage of experiment (i.e. finding appropriate joining direction) were fabricated by aforementioned parameter setting.

In order to evaluate the formability with respect to joining material direction, the AA6061 sheets were considered with three different types of material direction combinations: i.e. (1) both sheets were parallel to rolling direction (2) both sheets were perpendicular to rolling direction and (3) both sheets were diagonal to rolling direction and then welded under aforementioned FSW parameter setting. The joints with different directions are shown in Figs. 1c and 2c. After performing FSW under different material directions, the fabricated joints were then formed to bowl shape via single point incremental forming process to find which direction resulted in maximum formability i.e. maximum bowl height until failure occurs. The direction with higher bowl height (i.e. better formability) was considered as the main direction for performing next stages of experiment.

Also, a series of FSW tests were carried out to obtain forming limit curve of welded blank in incremental forming process. For this purpose, joints fabricated in different direction and under three different rotation speed

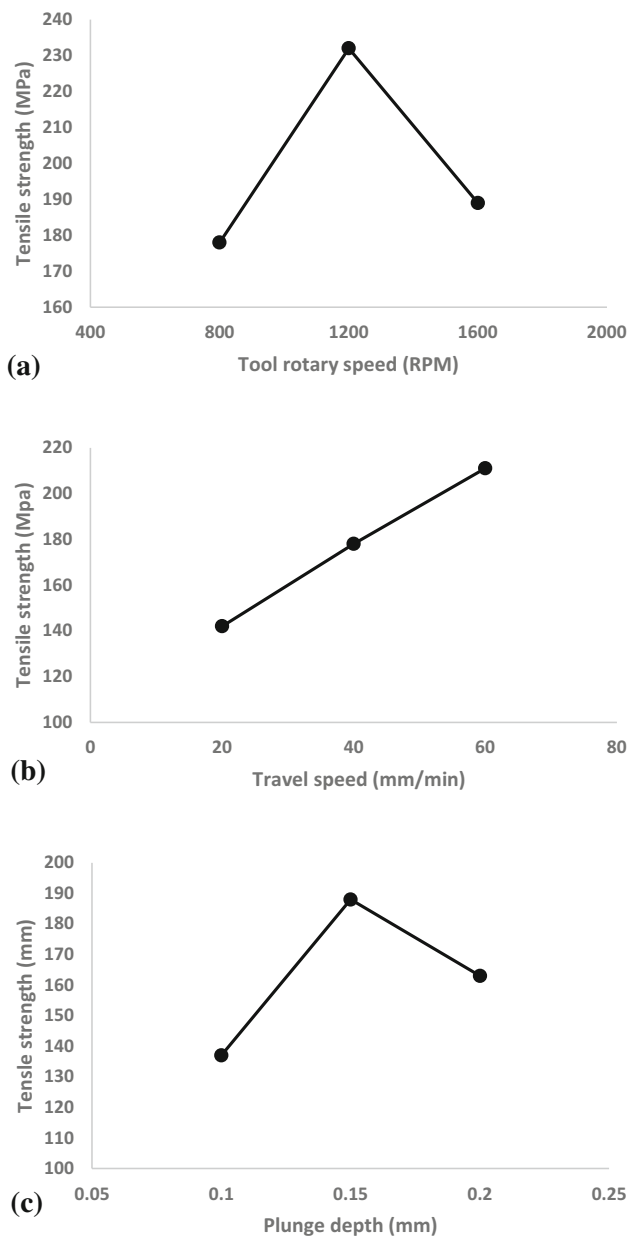


**Fig. 3** Effect of FSW process factors on joint strength

conditions simulating nine different predefined strain paths in stretching side were deformed to construct a forming limit curve (FLC). During the SPIF test, samples were first thoroughly cleaned with acetone to remove oil and dust particles from the sheet surfaces. Dot grids of diameter 2.5 mm were printed on the sheet surface. All the blanks were deformed until failure occurs. The true major strains and true minor strains of the ellipses, near the failure and away from the failure, were measured using a mylar strip ruler in all the strain paths. These major and minor strain data were plotted on a major strain ( $y$  axis)-minor strain ( $x$  axis) graph. The FLCs of the welded blanks were compared with each other to investigate the influence of the

joint direction on the forming limit strains of friction stir welded blanks.

Experiments in the second stage was aimed to find effects of FSW process factors on the formability of welded blanks that was formed via incremental forming process. Here experiments based on central composite design was carried out to find effects of tool rotary speed (800, 1000 and 1200 RPM), travel speed (40, 60 and 80 mm/min) and plunge depth (0.1, 0.15 and 0.2 mm) under three levels of formability. Also, in the third stage of experiments central composite design was also used to identify influence of spindle speed (0, 400 and 800 RPM), feeding rate (200, 400 and 600 mm/min) and axial step (0.2, 0.4 and 0.6 mm) on minimum thickness. In second and third stages of experiments, mathematical models of maximum bowl height and minimum thickness were developed, respectively; and parametric influence of factors on the responses were identified. Tables 3 and 4 presents effect of FSW factors on bowl height and SPIF factor on minimum thickness, respectively.

### 3 Results and Discussion

#### 3.1 Effect of Joining Material Direction and Relevant FLC

In this stage the welded blanks were fabricated by tool rotary speed of 1200 RPM, travel speed of 60 mm/min and plunge depth of 0.15 mm under three different joining directions. Then, the fabricated joints were subjected to incremental forming process with parameter setting of 400 RPM tool rotary speed, 400 mm/min feeding rate and 0.4 mm axial depth.

Effect of joining material direction on formability of the welded blanks are shown in Fig. 4a. It is seen from the figure that the blanks which have been joined in line with diagonal directions has higher formability than those joined perpendicular to rolling direction and those joined parallel to rolling direction. Effect of material direction on formability should be justified by use of strain-hardening exponent that is affected by plastic strain ratio of the sheet material. For evaluating this effect, tensile tests have been carried out taking into account different material joining direction. The results of tensile tests are presented in Fig. 4b. According to this figure, it is seen that the joint fabricated with orientation of  $45^\circ$  relative to rolling direction (i.e. diagonal direction) has higher strain hardening exponent ( $n$ -value) compared to joint fabricated with orientation of  $90^\circ$  relative to rolling direction (i.e. perpendicular to rolling direction) and that fabricated parallel to rolling direction. During metal forming process, the

**Table 3** Design matrix and obtained value of bowl height in the second stage of experiment

No.	N (RPM)	T (mm/min)	d (mm)	Minimum thickness (mm)
1	800	40	0.1	15
2	1600	40	0.1	42
3	800	80	0.1	11
4	1600	80	0.1	31
5	800	40	0.2	14
6	1600	40	0.2	36
7	800	80	0.2	14
8	1600	80	0.2	33
9	800	60	0.15	13
10	1600	60	0.15	26
11	1200	40	0.15	22
12	1200	80	0.15	15
13	1200	60	0.1	13
14	1200	60	0.2	13
15	1200	60	0.15	19
16	1200	60	0.15	20
17	1200	60	0.15	21
18	1200	60	0.15	20
19	1200	60	0.15	21
20	1200	60	0.15	20

**Table 4** Design matrix and obtained value of minimum thickness in the third stage of experiment

No.	S (RPM)	f (mm/min)	$\delta z$ (mm)	Minimum thickness (mm)
1	0	200	0.2	0.85
2	800	200	0.2	0.55
3	0	600	0.2	1.06
4	800	600	0.2	0.7
5	0	200	0.6	0.77
6	800	200	0.6	0.5
7	0	600	0.6	1.08
8	800	600	0.6	0.7
9	0	400	0.4	1.11
10	800	400	0.4	0.65
11	400	200	0.4	0.64
12	400	600	0.4	0.83
13	400	400	0.2	0.75
14	400	400	0.6	0.7
15	400	400	0.4	0.74
16	400	400	0.4	0.72
17	400	400	0.4	0.7
18	400	400	0.4	0.78
19	400	400	0.4	0.69
20	400	400	0.4	0.75

strain hardening exponent and plastic strain ratio values indicate stretchability and formability [17, 18]. As the  $n$ -value increases, the stretchability also increases and the material endures higher tensional stress during forming process. Therefore, sheets joined in diagonal direction has higher formability (i.e. bowl height) during incremental forming process. Hence, this direction has been used for conducting next stage of experiment.

To systematically analyze the effect of joining direction on formability of friction stir welded blank, FLC of the samples have been drawn according to threshold between safe and failed strain values. The forming limit curve for different joining direction is presented in Fig. 5. It is seen from the figure that joints fabricated at diagonal direction has highest formability than the others. According to strain hardening exponent obtained from tensile tests as shown in Fig. 5, the strain hardening coefficient for the joint fabricated at diagonal direction is higher than those fabricated parallel or perpendicular to rolling direction. The strain hardening coefficient influences the strain distribution in a forming operation. Increasing the  $n$  value distributes the strain and thickness uniformly in sheets during forming. If strain distribution is uniform, then FLC is likely to improve [13]. Also, it is inferred that joint which is fabricated in rolling direction has higher strain hardening coefficient compared to that fabricated parallel to the rolling direction. Therefore, according to abovementioned description, by increase in strain hardening coefficient, the strain distribution also enhances that causes improvement of FLC.

### 3.2 Mathematical Model of Bowl Height and Minimum Thickness

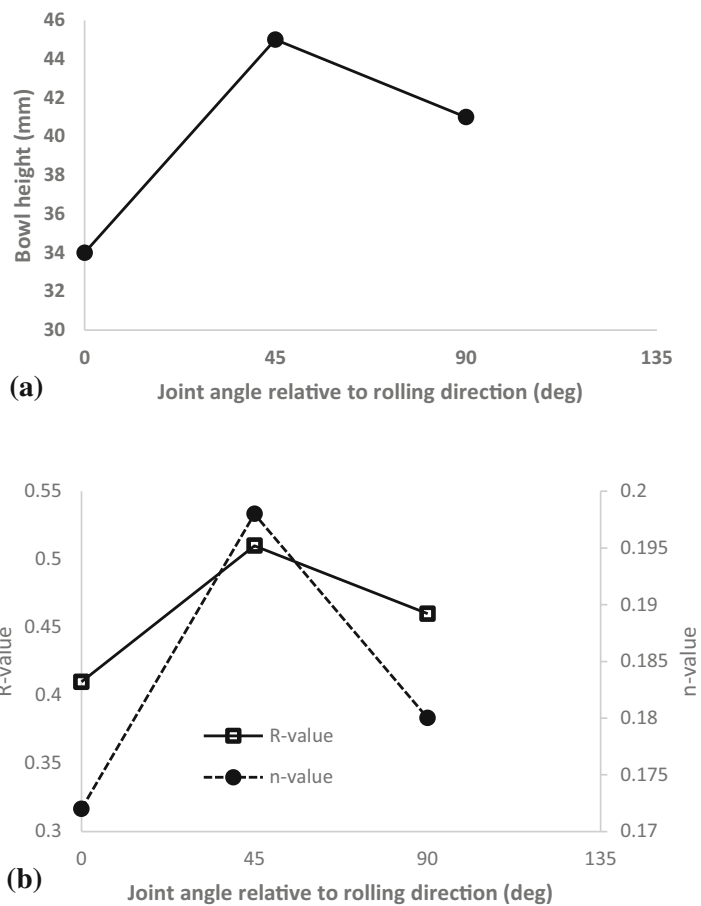
After conducting experiment based on design matrix of Tables 3 and 4, the maximum bowl height and minimum thickness are statistically modeled by using response surface methodology. Second-order mathematical models of bowl height and minimum thickness including linear, interaction and quadratic terms are presented in Eqs. 1 and 2, respectively.

$$\begin{aligned}
 h \text{ (mm)} = & 47.74 - 0.027N - 0.91T - 13.27d - 5.6 \\
 & \times 10^{-4}NT - 0.05Nd \\
 & - 1.5Td + 3.9 \times 10^{-5}N^2 + 0.013T^2 + 691d^2
 \end{aligned} \quad (1)$$

where  $h$  is maximum bowl height,  $N$  is tool rotary speed,  $T$  is travel speed and  $d$  is plunge depth.

$$\begin{aligned}
 Th \text{ (mm)} = & 0.8 - 2 \times 10^{-4}S - 2 \times 10^{-4}f + 0.36\delta z \\
 & + 4.6 \times 10^{-8}Nf - 2 \times 10^{-4}N\delta z + 2 \times 10^{-4}f\delta z \\
 & + 1.9 \times 10^{-7}N^2 + 5.2 \times 10^{-7}f^2 - 0.22\delta z^2
 \end{aligned} \quad (2)$$

**Fig. 4 a** Values of bowl height until failure under different joining direction, **b** R-values and n-value for different joining direction



where  $Th$  is the minimum thickness and  $S$ ,  $f$  and  $\delta z$  are spindle speed, feeding rate and axial step, respectively.

To check the adequacy of developed models, analysis of variance (ANOVA) for bowl height and minimum thickness has been performed and the results are given in Table 5 and 6. In ANOVA table, the model Prob > F value and lower than 0.05 implies that the model terms are significant. Also, the  $P$  value for the term of lack-of-fit higher than 0.1 implies that this term is insignificant. In addition, the coefficient of determination  $R^2$  is in good agreement with adjusted  $R^2$  and this implies high mathematical validity of regression functions. It is inferred that all the developed regression models are adequate enough to correlate exact relationship between process factors and corresponding responses. Also, it is inferred from the Table 5 that tool rotary speed is the most significant parameter affecting the maximum bowl height; while the feed rate has greatest impact on minimum thickness.

### 3.3 Effect of FSW Parameters on Bowl Height

In this section, effect of welding parameters on formability are analyzed. Here, the tool rotary speed, travel speed and plunge depth are varied over the ranges of 800–1600 RPM,

40–80 mm/min and 0.1–0.2 mm, respectively; and joints are fabricated along the diagonal direction. Also, all the incremental forming experiments are performed by parameter setting of 400 RPM tool rotary speed, 400 mm/min feeding rate and 0.4 mm axial depth. To analyze the results, the graphs developed by mathematical models are extracted from DESIGN EXPERT software and the behavior are discussed based on FSW process mechanism. Figure 6 illustrates effect of FSW parameters on bowl height including both the perturbation and 3D surface plots. According to this figure, the parametric influence is explained as follows.

#### 3.3.1 Effect of Tool Rotary Speed and Travel Speed

It is ascertained from the Fig. 6 that irrespective of travel speed, increase in tool rotary speed from 800 to 1600 RPM causes increase in formability. However, the value of bowl height decreases by increase in welding travel speed.

Before discussing the results, mechanism of heat generation and influential factors should be theoretically explained. According to Zhang [19], heat generation in the interface of tool and sheet is due to three sources: i) heat generation from the shoulder face i.e.  $W_1$ , ii) heat

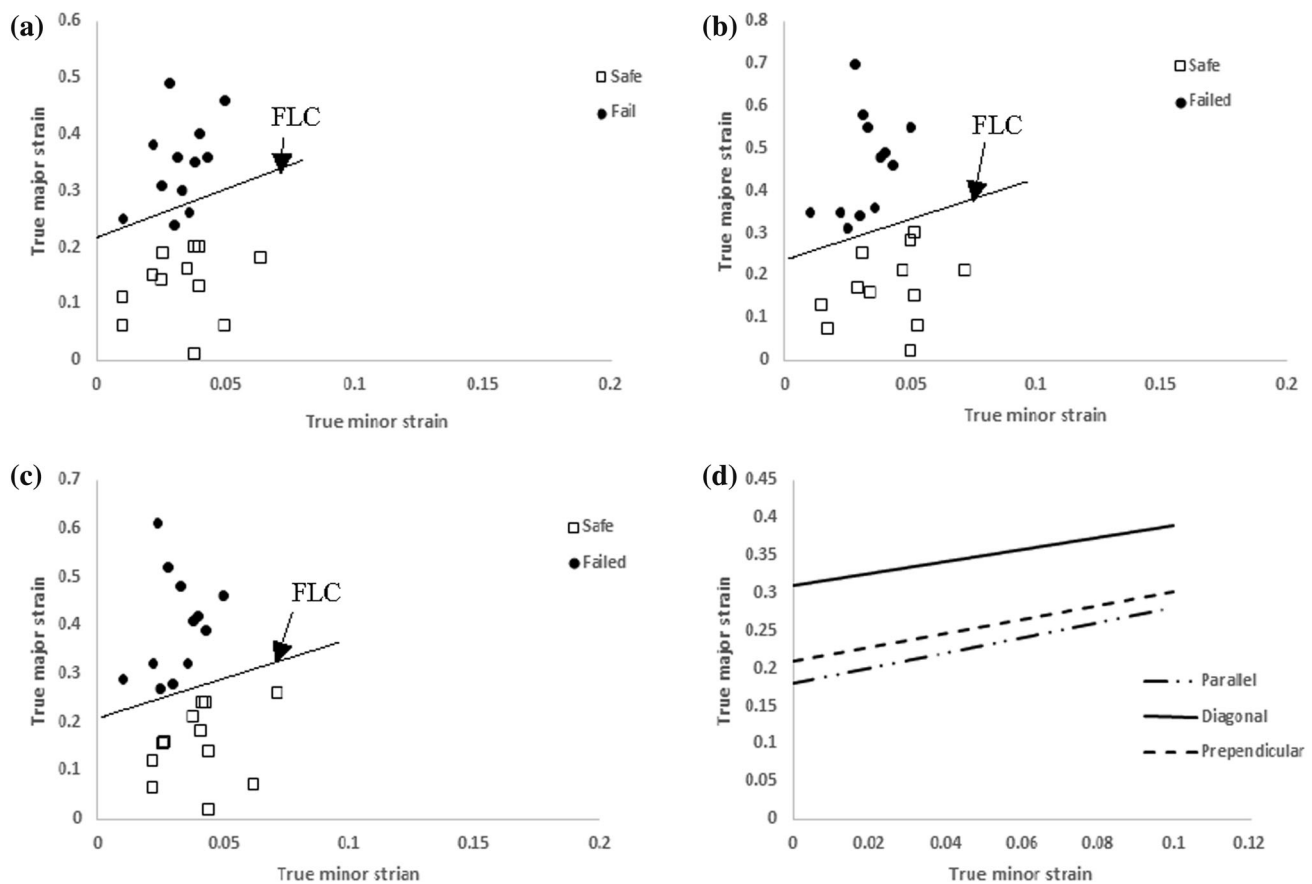


**Fig. 5** Forming limit diagram obtained for different joining direction. **a** Parallel, **b** diagonal, **c** perpendicular, **d** comparison of forming limit curve for different joining direction

generation from pin side i.e.  $W_2$  and iii) heat generation from pin face i.e.  $W_3$ . Following presents dependency of heat generation to processing parameters.

$$W_1 = \frac{3}{2} \pi \omega \mu P (R_{\text{shoulder}}^3 - R_{\text{pin}}^3) \quad (3)$$

$$W_2 = 2 \pi \omega \mu P R_{\text{pin}}^2 H_{\text{pin}} \quad (4)$$

$$W_3 = \frac{2}{3} \pi \omega \mu P R_{\text{pin}}^3 \quad (5)$$

where  $\omega$  is tool rotary speed,  $\mu$  is friction coefficient,  $P$  is pressure applied by plunging action,  $R_{\text{shoulder}}$  is shoulder diameter,  $R_{\text{pin}}$  is pin diameter and  $H_{\text{pin}}$  is the pin length.

According to the above explanations, during friction stir welding process, tool rotary speed and welding speed play predominant role in heat generation and heat transfer, respectively. They determine formation of friction stir processed zone and significantly affect macro microstructural evolution [20, 21]. Mechanical properties and fracture location is highly affected by these factors. Increase in tool rotary speed and decrease in travel speed induces higher heat input in FSP zone and saves the temperature in weld

nugget for longer time [21]. Therefore, both heat and time are provided for performing dynamic recrystallization. Under such condition, the microstructure of the weld is dynamically recrystallized and grain refining occurs in FSP zone and weld nugget. The coarse and non-uniform microstructure are diminished and fine, equiaxed and elongated grain distribution are formed in weld nugget. This results in improving formability and tear occurs at higher bowl height. Figure 7 presents the microstructure of the weld nugget and fractography of the torn surface under different combination of tool rotary speed and travel speed. It is inferred from the figure that microstructure of the weld nugget fabricated at high tool rotary speed and low travel speed (i.e. 1600 RPM and 40 mm/min) is finer and uniformly distributed with elongated shape. This causes improvement in ductility and enhances the formability of the TWBs. Also, the fractography analysis under aforementioned parameter setting shows that the fracture surface contains large and elongated dimples implying that the tear occurs at higher value of strain. On the other hand, the microstructure of the weld nugget produced under low tool rotary speed and high travel speed (i.e. 800 RPM and



**Table 5** ANOVA results of bowl height

Source	Sum of squares	Degree of freedom	Means of square	F-value	Prob > F	Significance
Model	2216	9	253.12	24.45	<0.0001	Significant
<i>N</i>	980	1	980	102	<0.0001	
<i>T</i>	240	1	240	25	0.0005	
<i>d</i>	48	1	48	5	0.0487	
<i>NT</i>	162	1	162	16.85	0.0021	
<i>Nd</i>	8	1	8	0.83	0.3831	
<i>Td</i>	18	1	18	1.87	0.2012	
<i>N</i> <sup>2</sup>	106	1	106	11.09	0.0076	
<i>T</i> <sup>2</sup>	75	1	75	7.82	0.0189	
<i>d</i> <sup>2</sup>	8	1	8	0.85	0.3774	
Residual	96	10	9.6	–	–	
Lack-of-fit	96	5	19.2	1.8	0.521	Not significant
$R^2 = 0.9565$		$R^2_{adjusted} = 0.9174$			$R^2_{predicted} = 0.9321$	

**Table 6** ANOVA results of minimum thickness

Source	Sum of squares	Degree of freedom	Means of square	F-value	Prob > F	Significance
Model	0.47	9	0.052	28.78	<0.0001	Significant
<i>S</i>	0.31	1	0.31	172.73	<0.0001	
<i>f</i>	0.11	1	0.11	61.95	<0.0001	
$\delta z$	$2.5 \times 10^{-3}$	1	$2.5 \times 10^{-3}$	1.41	0.2623	
<i>Sf</i>	$3.61 \times 10^{-3}$	1	$3.61 \times 10^{-3}$	1.95	0.1885	
<i>S</i> $\delta z$	$1.25 \times 10^{-5}$	1	$1.25 \times 10^{-5}$	$6.89 \times 10^{-3}$	0.9355	
<i>S</i> $\delta z$	$2.81 \times 10^{-3}$	1	$2.81 \times 10^{-3}$	1.55	0.2414	
<i>S</i> <sup>2</sup>	0.035	1	0.035	19.11	0.0014	
<i>f</i> <sup>2</sup>	$2.94 \times 10^{-3}$	1	$2.94 \times 10^{-3}$	1.62	0.2314	
$\delta z^2$	$5.02 \times 10^{-3}$	1	$5.02 \times 10^{-3}$	2.77	0.1271	
Residual	0.018	10	0.018	–	–	
Lack-of-fit	0.013	5	$2.5 \times 10^{-3}$	2.24	0.986	Not significant
$R^2 = 0.9628$		$R^2_{adjusted} = 0.9294$			$R^2_{predicted} = 0.8103$	

80 mm/min) causes formation of coarse and non-uniform grain distribution that damages the formability of the TWBs. This is due to low heat input and lack of enough time for occurrence of dynamic recrystallization during FSW process. Fractography analysis in Fig. 7 shows that fracture surface contains no dimple and coalescence that implies tear has occurred at lower strains. However, at mediocre values of tool rotary speed and travel speed (i.e. 1200 RPM and 60 mm/min), the heat generation is moderate and a short time is provided for dynamic recrystallization, therefore the relevant microstructure is semi-fine and the fracture surface contains small dimples and coalescence to some extent. This microstructure and fractography results show that the tear occurs at strain value not high as in the former condition.

### 3.3.2 Effect of Tool Rotary Speed and Plunge Depth

Figure 6 demonstrates effect of plunge depth and tool rotary speed on bowl height i.e. formability of TWB. It is seen from the figure that when the plunge depths are 0.1 and 0.15 mm, the formability increases by increase in tool rotary speed. However, when the plunge depth is 0.2 mm, formability decreases by increase in tool rotary speed. Furthermore, it is ascertained from the Fig. 6 that irrespective to tool rotary speed, the formability firstly increases by increase in plunge depth from 0.1 to 0.15 mm. However, by further increase in plunge depth from 0.15 to 0.2 mm, the formability of TWB drastically, decreases.

During friction stir welding process, heat generation is significantly affected by applied pressure of tool on the

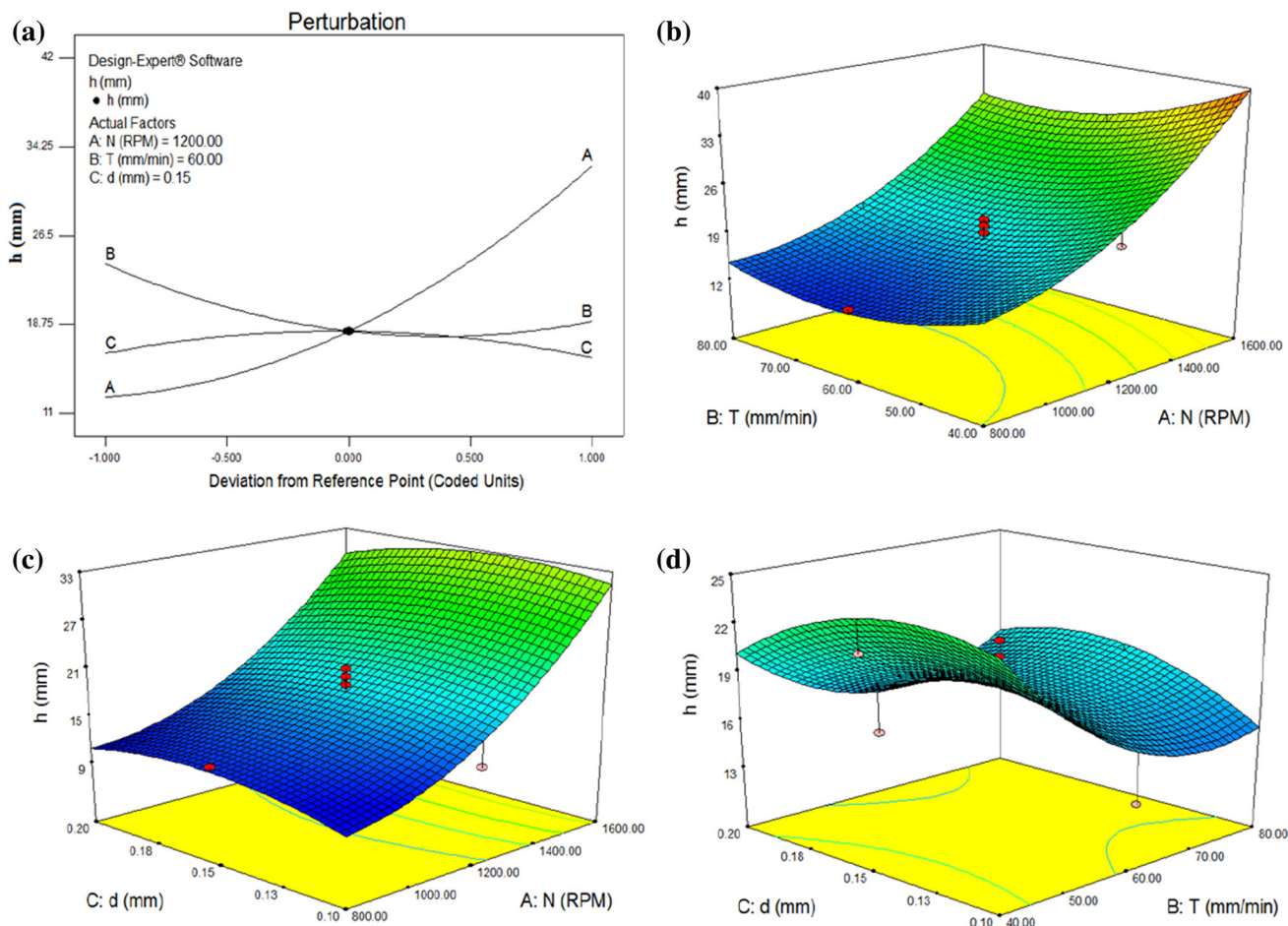


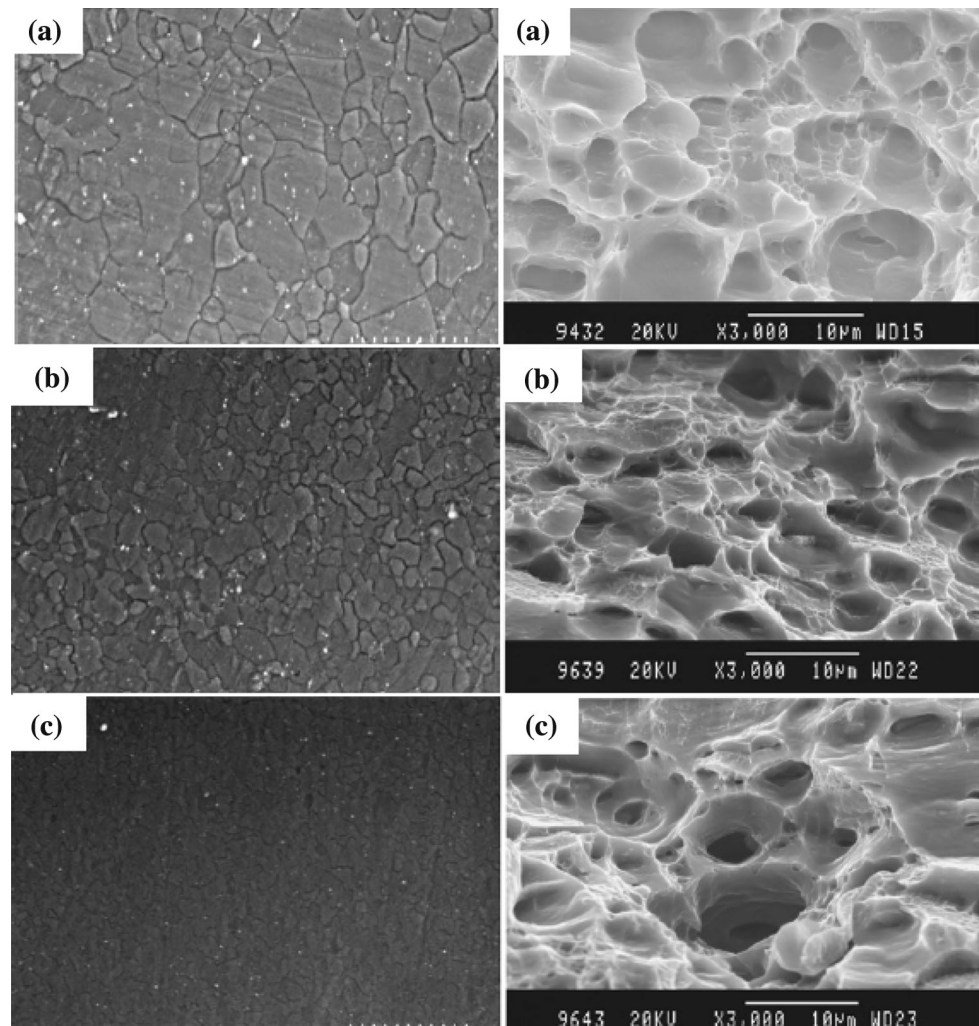
**Fig. 6** Effect of FSW factors on bowl height. **a** Perturbation plot, **b** interaction of spindle speed and feeding rate, **c** interaction of spindle speed and step down, **d** interaction feeding rate and step down

joint [19]. On the other hand, the pressure is provided by plunging action of the tool. Hence higher values of plunge depth causes more pressure and results in higher heat input. When the plunge depth increases from 0.1 to 0.15 mm, irrespective of tool rotary speed, due to increase in applied pressure, the heat input also increases and it causes dynamic recrystallization. In such condition, the microstructure of the weld nugget becomes refined and uniform with elongated shape. Subsequently, the ductility is improved and the bowl height increases until tear occurs. However, in 0.2 mm plunge depth, due to excessive increase in applied pressure, the thickness of the sheet subjected to plunging action decreases. Therefore, under such condition, the strength of the joint decreases and it causes failure at lower strains.

Figure 8 demonstrates macrostructure, microstructure and fracture surface of the joints fabricated under different parameter combination. When the plunge depth is 0.1 mm and tool rotary speed is 1600 RPM, the heat input is low and dynamic recrystallization occurs inappropriately due to low plunge depth. Under such condition, the

ductility is restricted. Thus, the grain distribution is coarse and fracture surface doesn't include large dimples. Also, the macrostructure of the FSP region contains a tunnel like defect that limits both the strength and formability. On the other hand, when the tool rotary speed is 1600 RPM and plunge depth is 0.15 mm, the heat input is sufficient that causes the weld nugget to dynamically recrystallize with uniform grain distribution. Therefore, ductility increases and fracture surface contains large and wide dimples. Also, the macrostructure has regular and defect-free form with sufficient material flow. In addition, when the tool rotary speed is 1600 RPM and plunge depth is 0.2 mm, the heat input is sufficient. Thus, dynamic recrystallization occurs and microstructure becomes uniform. However, due to reduction in thickness of the sheet at high plunge depth, the material weakens and defect like pin hole is formed along thickness direction. Under such condition, during incremental forming process, tear occurs at low forming height. Therefore, fracture surface contains no dimple implying failure occurring at lower strain values.

**Fig. 7** Microstructure and fracture surface of the joints produced under different tool rotary speed and travel speed, **a** 800 RPM and 80 mm/min, **b** 1200 RPM and 60 mm/min **c** 1600 RPM and 40 mm/min, the plunge depth is 0.15 mm



### 3.3.3 Obtaining Optimal FSW Parameter Setting for Maximum Bowl Height

Desirability approach function has been utilized here to obtain the optimal setting of FSW factors regarding maximum bowl height. The approach is suitable for solving both the single-objective and multi-objective optimization problem by combining multiple responses into a dimensionless measure of performance called the overall desirability function [22]. However, in the present investigation, the optimization has been performed only for a single response namely bowl height. According to the FSW parameter range, the parameter setting for maximum bowl height has been obtained and presented in Table 7. According to the table, it is found that the setting of 1600 RPM tool rotation, 40 mm/min travel speed and 0.15 mm plunge depth is the most optimal solution that helps in attaining maximum bowl height with a desirability of 100%.

According to the above results and relevant discussions, it is found that the setting of 1600 RPM tool rotary speed, 40 mm/min welding speed and 0.15 mm plunge

depth is an optimum combination of welding parameter. Experiment has been performed with the optimum parameter setting and the corresponding bowl height thus obtained is 52 mm.

### 3.4 Effect of SPIF Parameters on Minimum Thickness

For this stage of experiment, in order to analyze effect of incremental forming process factors on thickness distribution analysis, all the TWBs are fabricated with obtained optimal welding parameters (i.e. 1600 RPM tool rotary speed, 40 mm/min travel speed, 0.15 mm plunge depth and diagonal direction) and they are formed until 40 mm bowl height is achieved. The reason for selection of 40 mm height is to produce bowls with no failure for analyzing the thickness distribution. In other word, during thickness distribution analysis, the formed parts should contain no failure such as tear, buckling and wrinkling. However, to analyze effect of incremental forming parameters on the thickness distribution of the TWBs, the spindle speed,

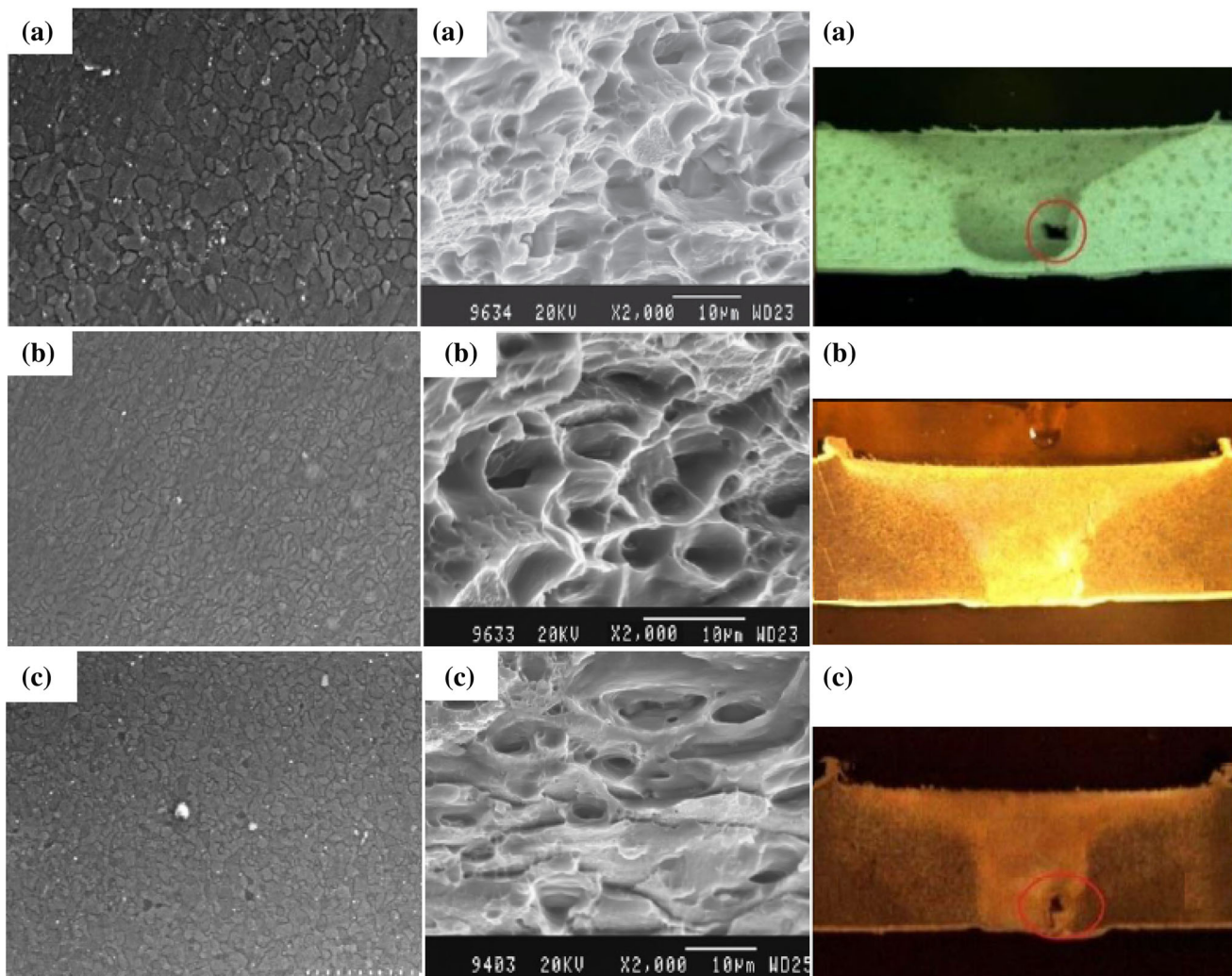


**Fig. 8** Microstructure, fracture surface and macrostructure of the joints produced under different tool rotary speed and plunge depth, **a** 1600 RPM and 0.1 mm/min, **b** 1600 RPM and 0.15 mm, **c** 1600 RPM and 0.2 mm

**Table 7** Optimal FSW parameter setting obtained by Design Expert based on identified criterion for maximum bowl height

Optimal setting			Responses	
N (RPM)	T (mm/min)	d (mm)	h (mm)	Desirability (%)
1600	40	0.15	54	100

feeding rate and axial depth are varied over 0–800 RPM, 200–600 mm/min and 0.2–0.6 mm, respectively. The graphs for parametric influence have been extracted according to Eq. 6 by means of DESIGN EXPERT statistical package. The effect of SPIF parameters on minimum thickness is described as follows.

### 3.4.1 Effect of Spindle Speed

Figure 9 demonstrates the effects of SPIF parameters on minimum thickness of the incrementally formed TWB. It is

seen from the figure that by increase in spindle speed, the minimum thickness decreases. In other word, the bowl that is incrementally formed by 0 RPM tool rotary speed has highest thickness distribution followed by bowls formed by 400 and 800 RPMs rotary speed. When the spindle speed increase, the temperature in contact zone between the tool and the sheet also increases. According to Fig. 10a, results obtained through temperature measurement show that an increase in spindle speed causes increase in temperature in the interface of tool and sheet. This rise in temperature causes the sheet material to be tensioned and causes thickness reduction [23].

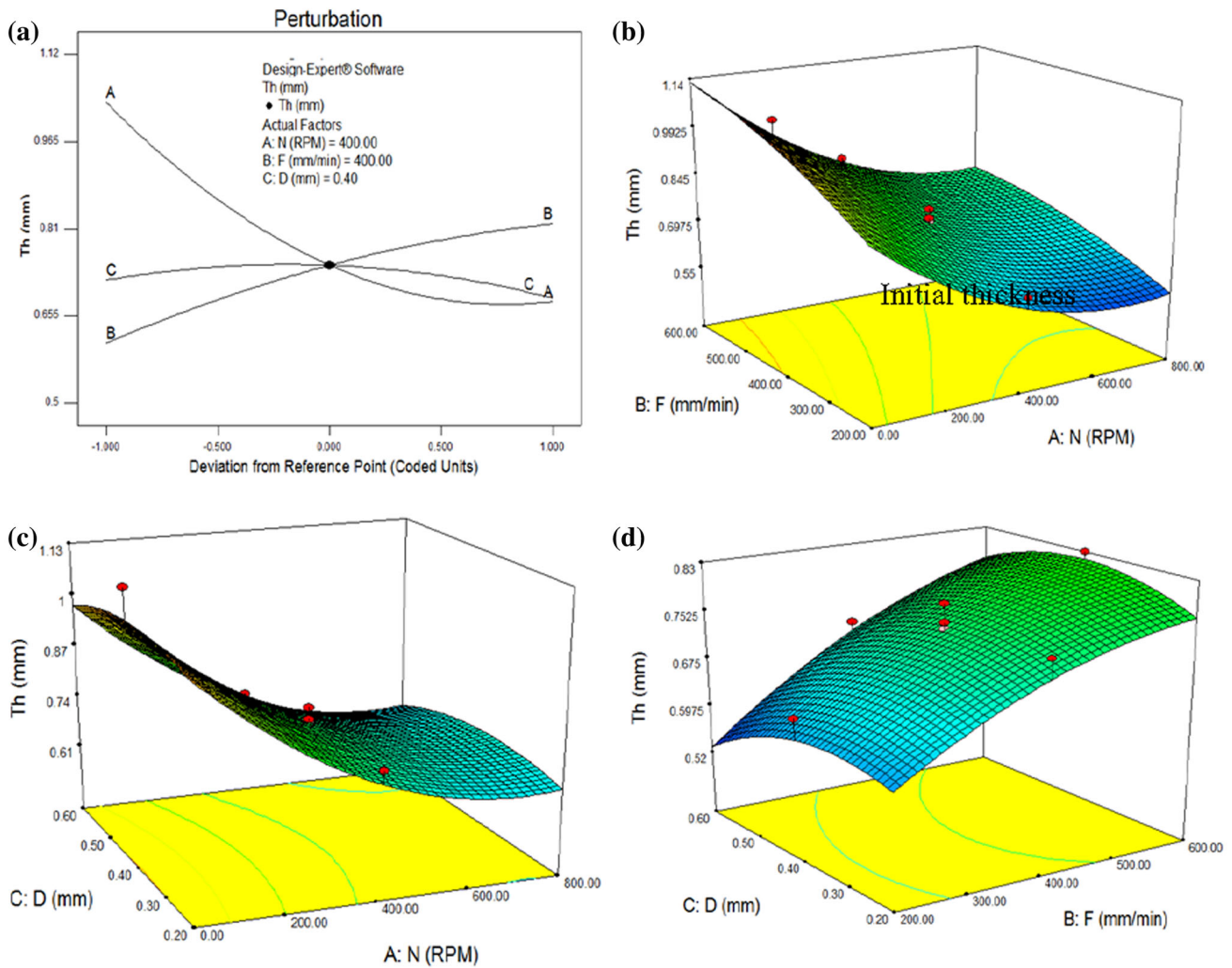


**Fig. 9** Effect of SPIF factors on minimum thickness, **a** perturbation plot, **b** interaction of spindle speed and feeding rate, **c** interaction of spindle speed and step down, **d** interaction feeding rate and step down

However, due to increase in forming temperature, formed material softens and forming force decreases (Fig. 10a). Reduction of forming force prevents work hardening effect and limits the stretchability of material. In other word, both rise in temperature and prevention from work hardening, which is caused by high tool rotary speed, results in reduction of minimum thickness.

### 3.4.2 Effect of Feeding Rate

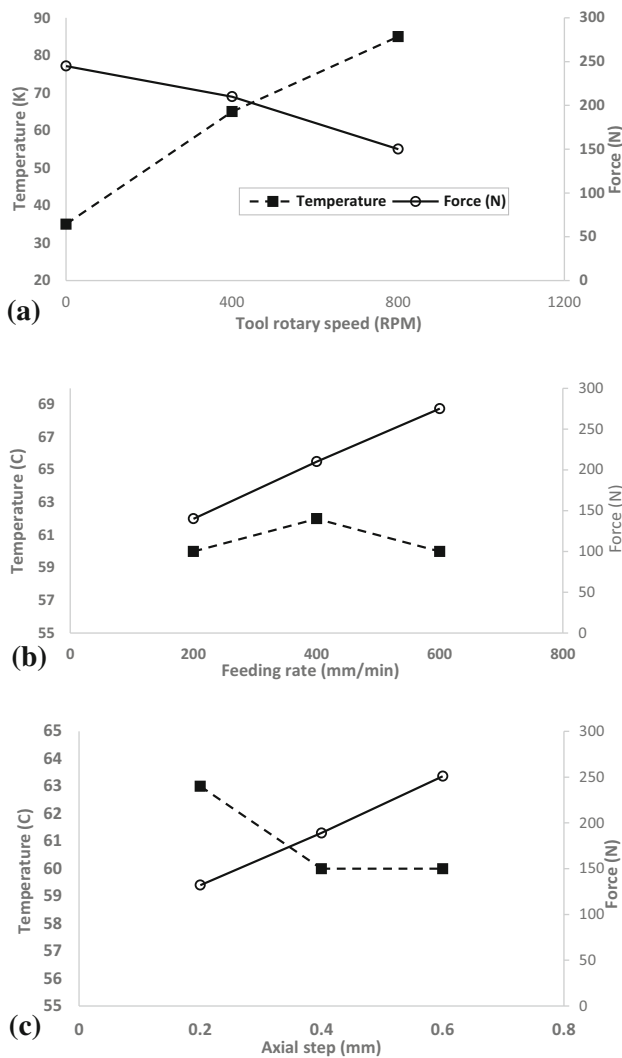
To find the effect of feeding rate on thickness distribution, the parameter is varied over levels of 200, 400 and 600 mm/min and other parameters such as spindle speed and axial depth are kept constant at 400 RPM and 0.4 mm, respectively.

Figure 8 demonstrates minimum thickness of formed parts under different feeding rate. It is inferred from the figure that by increase in feeding rate, the thickness distribution enhances. When the feeding rate increases, the

forming force increases subsequently (Fig. 10b). This is due to the fact that at high feeding rate, more material is formed by the movement of a tool in a given path. Hence, due to increase in forming force, the formed material is work-hardened and the strength of the sheet increases. Under such condition, the sheet resists against tensional stress and the thickness distribution enhances [24]. Figure 10b also, indicates variation of forming temperature under different feeding rate. It is seen from the figure that the temperature in the tool-sheet interface does not vary with the variation of feeding rate, significantly. Therefore, the forming force is the most significant factor affecting strain hardening and improves the thickness distribution.

### 3.4.3 Effect of Axial Step

To find the effect of axial step on thickness distribution, the parameter is varied over levels of 0.2, 0.4 and 0.6 mm and other parameters such as spindle speed and feeding



**Fig. 10** **a** Variation of temperature and resultant force versus variation of tool rotary speed, **b** variation of temperature and resultant force versus variation of feeding rate, **c** variation of temperature and resultant force versus variation of axial step

rate are kept constant at 400 RPM and 400 mm/min, respectively.

Figure 8 demonstrates thickness distribution of the formed parts under different axial step. It is inferred from the figure that by increase in axial step. The thickness distribution improves. When the axial step increases, the tool and sheet engagement also increases and it causes the tool be able to form more material during each given path. Under such condition, the value of forming force increases (Fig. 10c) and causes the sheet metal to be work-hardened [25]. Under such condition, the material strength against tensional stresses enhances and the thickness distribution improves. In addition, Fig. 10c illustrates variation of forming temperature under different axial depth. It is seen from the figure that the contact temperature doesn't vary with the variation of axial step. Therefore, the forming

force is the most significant factor affecting strain hardening. Increase in the force caused by higher axial step enhances the thickness distribution.

#### 3.4.4 Obtaining Optimal SPIF Parameter Setting for Maximum Critical Thickness

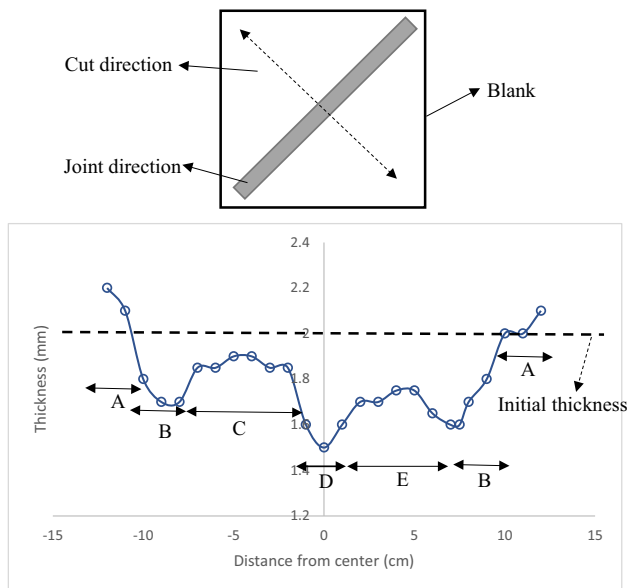
Desirability approach function has also been used here to maximize the minimum thickness of the formed sample. The identified criteria of process factors are 0–800 RPM spindle speed, 200–600 mm/min feed rate and 0.2–0.6 mm axial depth. According to this range the parameter setting for highest minimum thickness is obtained and presented in Table 7. It is found from the table that incremental forming parameter combination of 0 RPM spindle speed, 600 mm/min feeding rate and 0.6 mm axial depth is the most optimum parameter setting that causes attainment of 1 mm critical thickness with desirability of 100% (Table 8).

Therefore, an experiment with obtained optimal setting is carried out and the thickness profile is represented in Fig. 11. From the figure, it is seen that the thickness distribution is apparently close to that of initial thickness. Also, the average thickness at optimum level is 1.76 mm that is 85% of initial thickness. It is worth mentioning here that the minimum thickness in the optimized sample is approximately 1 mm, that shows enhancement of part quality by performing optimization.

Figure 11 shows thickness distribution along with cutting direction for specimen fabricated and formed under optimum parameter setting. It is clear that the thickness distribution is characterized by five zones i.e. A, B, C, D and E. The zones characterized by A, are flange where the thickness is higher than that of initial material. The zones characterized by B are wall of the bowl, where the material experience both tensional and flexural stress. Hence, the thickness values in these zones decreases due to biaxial stress mode. The zone D is in the weld nugget that is subjected to pressure from the tool; therefore, the thickness value of this zone is lower than other sides. The zone C is in retreating side (according to welding direction) and the zone E is in advancing side. It is seen that the value of thickness zone E is lower than that of zone C. This is because, the thermal gradient and the temperature field in the advancing side is relatively higher than that of retreating side [26]. The recorded temperature shows that during welding process (at optimal parameter setting), the temperature in retreating side is 103 °C while in the advancing side, the temperature is 171 °C. Hence, during incremental forming process the advancing side is subjected to more tensional stress and the thickness distribution decreases. The results are in line with the findings of Ramalu et al. [13].

**Table 8** Optimal SPIF parameter setting obtained by Design Expert based on identified criterion for highest minimum thickness

Optimal setting			Responses	
S (RPM)	F (mm/min)	$\delta z$ (mm)	Th (mm)	Desirability (%)
0	600	0.6	1	100

**Fig. 11** Thickness distribution at optimal level i.e. 0 RPM tool rotary speed, 600 mm/min feeding rate and 0.6 mm axial depth

## 4 Conclusion

In the present work, an experimental study was performed to analyze the formability of AA6061 friction stir welded blank through single point incremental forming. The TWBs were formed in the shape of bowl and its height (until tear occurred) was characterized as formability. Effect of joining material direction and FSW process parameters on bowl height was analyzed. After finding optimal welding parameters, all the TWBs were fabricated based on the optimum welding parameters and subjected to incremental forming process to analyze the effect of forming parameters on thickness distribution. Obtained results can be summarized as follows.

- Analysis of joining material direction showed that the joints fabricated via diagonal direction had highest formability i.e. 46 mm. The transverse direction and rolling direction had formability of 41 and 35 mm, respectively.
- The main reason for enhancing the formability in diagonal direction was its strain-hardening coefficient i.e. 0.198, which was higher than that of transverse direction with 0.17 n-value and rolling direction with 0.14 n-value.

- From the results, it was found that selection of 1600 RPM tool rotary speed, 40 mm/min travel speed and 0.15 mm plunge depth resulted in maximum formability i.e. 52 mm. The microstructure of the weld nugget at this parameter setting was completely fine and uniform with equiaxed and elongated grain distribution. Also, the fracture surface contained large and wide dimples implying fracture occurred at higher plastic strains.
- The maximum thickness distribution was obtained when the incremental forming parameters were 0 RPM spindle speed, 600 mm/min feeding rate and 0.6 mm axial depth. Average thickness distribution with this parameter testing was 1.77 mm that was 85% of base material.
- From thickness distribution, it was found that the thickness in the flange zone was maximum. Also, the weld nugget and wall zones had lowest thickness values.
- In addition, the thickness distribution in the advancing side was about 22% lower than that in the retreating side. According to Zhang et al. [26] and Ramalu et al. [13], the thermal gradient in advanced zone was relatively higher, that caused more tensional stress. Therefore, the thinning on that side was higher.

## References

1. Davies R W, Grant G J, and Oliver H E, *Metall Mater Trans A* **32** (2001) 275.
2. Saunders F I, and Wangoner R H, *Metall Mater Trans A* **27** (1996) 2605.
3. Davies R W, Oliver H E, Smith M T, and Grant G J, *JOM* **51** (1999) 46.
4. Sato S Y, Kokawa H, Enomoto M, and Johan S, *Metall Mater Trans A* **30** (1999) 2605.
5. Sato Y S, Kokawa H, Enomoto M, and Johan S, *Metall Mater Trans A* **30** (1999) 3125.
6. Mahoney N W, Rhodes C G, Flintoff J G, Bingel H W, and Spurling R A, *Metall Mater Trans A* **29** (1998) 1955.
7. Elangovan K, and Balasubramanian V, *Int J Adv Manuf Technol* **38** (2008) 285.
8. Zeng W M, Wu H L, and Zhang J, *Acta Metall Sin* **19** (2006) 9.
9. Lee W B, Yeon Y M, and Jung S B, *Mater Trans* **45** (2004) 1700.
10. Sato Y S, Sugiura Y, Shoji Y, Park S H C, Kokawa H, and Ikeda K, *Mat Sci Eng A* **369** (2004) 138.
11. Hirata T, Oguri T, Hagino H, Tanaka T, Chung S W, Takigawa Y, and Higashi K, *Mat Sci Eng A* **456** (2007) 344.
12. Kim D, Lee W, Kim J, Kim C, and Chung K, *Int J Mech Sci Eng* **52** (2010) 612.
13. Ramalu P J, Narayanan R G, and Kailas S V, *Int J Adv Manuf Technol* **69** (2013) 2757.
14. Ahmadnia M, Seidnalo A, Teimouri R, Rostamiyan Y, and Tirtash K H, *Int J Adv Manuf Technol* (2015). doi: [10.1007/s00170-015-6784-0](https://doi.org/10.1007/s00170-015-6784-0).
15. Silva M B, Skjodet M, Vilaca P, Bay N, and Martins P A F, *J Mater Proc Technol* **209** (2009) 811.
16. Babajanzade S, Behboodi-Jooybari M, Teimouri R, Asgharzade-Ahmadi S G H, Falahati-Naghbi M, Sohrabpoor H, *Int J Adv Manuf Technol* **69** (2014) 1803.

17. Narayanasamy R, Parthasarathi N L, and Sathiya Narayanan C, *Mater Des* **30** (2009) 1310.
18. Narayanasamy R, Ravi chandran M, Sathiya Narayanan C, Parthasarathi N L, and Ravindran R, *Int J Mech Mater Des* **3** (2006) 293.
19. Zhang Z, *J Mater Sci* **43** (2008) 5867.
20. Elangovan K, Balasubramanian V, and Babu S, *Mater Des* **30** (2009) 188.
21. Rajakumar S, Muralidharan C, and Balasubramanian V, *Mater Des* **32** (2011) 535.
22. Rajakumar S, Muralidharan C, and Balasubramanian V, *Mater Des* **32** (2011) 2878.
23. Lang L, Danckert J, and Nielsen K B, *J Mater Proc Technol* **148** (2004) 119.
24. Chang Q F, Li D Y, Peng Y H, and Zeng X Q, *Int J Mach Tools Manuf* **47** (2007) 436.
25. Gorji A, Alavi-Hashemi H, Bakhshi-Jooybari M, Nourouzi S, and Hosseinipour S J, *Int J Adv Manuf Technol* **56** (2011) 915.
26. Zhang Z, and Zhang H W, *Int J Adv Manuf Technol* **72** (2014) 1647.